2015-01-01

Hydrodynamic Cavitation as a Method for Cell Disruption

Christopher Caviglia
University of Texas at El Paso, ckcaviglia@miners.utep.edu

HYDRODYNAMIC CAVITATION AS A METHOD FOR CELL DISTRUPTION

CHRISTOPHER CAVIGLIA

Department of Mechanical Engineering

APPROVED:

_____
Russell Chianelli, Ph.D., Chair

_____
Norman Love, Ph.D.

_____
Barry A. Benedict, Ph.D.

_____
Charles H. Ambler, Ph.D.
Dean of the Graduate School

For my family.

HYDRODYNAC CAVITATION AS A METHOD FOR CELL DISRUPTION

By

CHRISTOPHER CAVIGLIA, B.S.M.E.

THESIS

Presented to the Faculty of the Graduate School of

The University of Texas at El Paso

in Partial Fulfillment

of the Requirements

for the Degree of

MASTER OF SCIENCE

Department of Mechanical Engineering

THE UNIVERSITY OF TEXAS AT EL PASO

December 2015

Acknowledgements

I would first like to thank my dear friend Joaquin Rodriguez for introducing me to the field of sustainable research. By extension, I must thank Dr. Gary Hawkins for many years of dedication and inspiration to his students.

I want to thank Dr. Russel Chianelli for allowing me to pursue this project, as well as his patience and willingness to aide me in seeing this project through to the end. Thanks also to everyone at the Materials Research and Technology Institute who have helped whenever I needed it.

Thank you also to Dr. Rastegary and Tracey Fernandez with New Mexico State University's Institute for Energy and the Environment for continually providing me with samples of algae.

Lastly, I would like to thank my family, who has been my main support system and motivation to further my education.

Abstract

Development of new renewable technologies is an important driver in the scientific community. As atmospheric carbon dioxide levels increase and the dependence on a finite amount of fossil fuel remains, the need for sustainable forms of energy is ever growing. Research in the field of renewable biofuels has pointed researchers toward the naturally occurring, robust, lipid-producing microorganism; microalgae. Its ability to sequester carbon and yield high lipid production has made it very attractive to renewable research. It has the potential to produce up to 10 times the oil, per acre, than competing biofuel feedstocks. However, an energy efficient method of harvesting algal biomass has yet to be utilized. The methods currently used employ large energy inputs, reducing overall efficiency of the harvest. The use of cavitation as destructive phenomenon has been largely studied in the past as something to avoid. Problems encountered on boat propellers, pump impellers, and turbines are designed to stay within certain operating parameters as to avoid cavitation, which would lead to failure of the equipment. It has more recently gained attention as a useable force, however a more thorough investigation of cavitational parameters is required in order to aid engineers and designers to understand the extent of its usefulness. The work implements a hydrodynamic cavitation system testing different operating parameters for evaluation of efficiency. Orifice plates were tested at varying cavitation numbers, power inputs, and geometric parameters in a controlled system. The Weissler reaction was employed to verify the intensity of the cavitating flow and the influence of tested parameters. Efficiency comparable to current cavitation extraction methods was achieved. Wet algal biomass samples were then run through the reactor to verify the effect of cavitation on cell wall disruption.

Table of Contents

List of Figures

Chapter 1

Introduction

Research in renewable and sustainable alternatives to fossil fuels has gained much interest over the past 30 years. This research has become increasingly prevalent in the past decade. Research to discover and develop sustainable forms energy is growing on a yearly basis. The use of oil as a source of energy over the last hundred years has increased significantly with the US consuming 18.878 million barrels of oil daily in 2013, which is 19.9% of world oil consumption, at only 4.5% of the world's population. Total world oil consumption is now at 91.33 million barrels per day (*BP; 2014*). It is apparent that these consumption levels are not sustainable, creating a need for research and implementation of alternative forms of energy. There is promising research across various fields focused around creating a viable solution to this problem. Of the three physical forms of fuel energy, solid, liquid and gaseous; liquid based fuels are the most energy dense form of fuel. Lipids derived from algal species offer an interesting alternative to fossil fuels and coal, not only as a renewable biofuel source but also as a form of energy generation that aids in closing the carbon loop. The use of lipids, through extraction and conversion, has become one of the most researched topics in biofuel feedstocks.

The need for research across the broad field of biofuels is justified in Chapter one of this text through the exploration of liquid based fuels, their impact, and their limitations. The consumption of fossil fuels throughout the world is explored economically, environmentally, and quantitatively. The justification continues through investigation and a brief overview of biofuels in general; their viability as well as drawbacks. Finally an argument for the use of algae as a biofuel is made, highlighting the prospects of this energy source.

Chapter 2 explores the use of algae as an alternative form of biofuel. An understanding of the base organism must first be achieved. Growth mechanisms and characteristics of different strains of algae is then compared. Techniques and other growth inputs of a bio-reactor system are also examined to explore the scalability algal growth. Finally, the various extraction methods are reviewed, giving adequate justification for the exploration of cavitation as a method for cell disruption.

Cavitation can be described, in a closed hydraulic system, as the inception, growth and collapse of a bubble within the fluid medium. Cavitation is incited hydrodynamically, through a large pressure drop in the system created, in this case, by an orifice plate. The holes in the orifice plate restrict the flow area to a fraction of the total pipe diameter, increasing velocity of the flow through the orifice, a trade off of the permanent pressure loss. The velocity increase will then form a liquid jet downstream of the orifice. This submerged liquid jet causes shear within the fluid, causing cavitation. As the pressure recovers downstream, the cavities will then collapse, giving rise to high intensity temperatures and pressures that can be utilized to cause physical and chemical changes to the system.

To better understand the potential for cavitation as an energy efficient form of cell lysis, an exploration into hydrodynamic cavitation is performed. Section 3 then, will focus on cavitation itself; investigating both physical and chemical effects of the process to be utilized. The basis for understanding cavitating flow is formed and key parameters are introduced, as well as proposal for a new parameter created as a result of this work, whose purpose is to aid in the scalability of this process. The experimental process is then outlined, providing the systematic approach and methods used throughout the project. This will encompass the entire design of the

experiment, including the experimental apparatus and the method by which cavitation is quantified.

This thesis is undertaken in order to explore the feasibility of the utilization of hydrodynamic cavitation to lyse algal biomass in its wet form, thereby reducing the cost of the extraction process. The experiment is done at a pilot scale in an attempt to justify the scalability and use of this technology for future applications and potential further implementation.

1.1 The Need for Energy Alternatives

Oil consumption worldwide is ever growing, and the human dependence on fossil fuels is highly unsustainable, both to the availability of the resource as well as the effect its consumption has on our planet via emissions. Subsidies and tax breaks for sustainable energy companies' relays the need and the willingness of the government to support such projects. This interest in renewables stems from those problems forecast on the horizon and those directly at our doorstep. As of the year 2011, greenhouse gasses (GHG's) carbon dioxide (CO2), methane (CH4) and nitrous oxide (N20) surpassed pre-industrial levels of 40%, 150%, and 20%, respectively (ICCP, 2013). Global temperatures are projected to increase significantly in the coming century, leading to a number of problems, foreseeable and not.

Another important consideration is total oil consumption. In 2013, consumption and production of fuels, aside from nuclear energy, saw all time highs. Annual global energy consumption in million tonnes of oil equivalent (mtoe) totaled 12,730.4 and growth in global primary energy consumption was estimated at 2.3%, for the year 2014. Oil was consumed at 4185.1 mtoe, 32.87% of total energy consumption. Meanwhile, biofuel consumption saw a 6.1% increase in 2013, the highest increase since 2008 (*BP; 2014*). Continually increasing consumption coupled with a finite amount of oil reserve inevitably creates a very volatile and

factor dependent market for the price of oil. The total of world oil reserves in 2013 is estimated at 1,687.9 billion barrels of oil. As a function of our production, the current world reserves are estimated to meet only 53.3 more years of global production according to the 2014 BP Statistical Review of World Energy. The ratio of current reserves to production for 2013 by region can be seen in Figure 1, below.

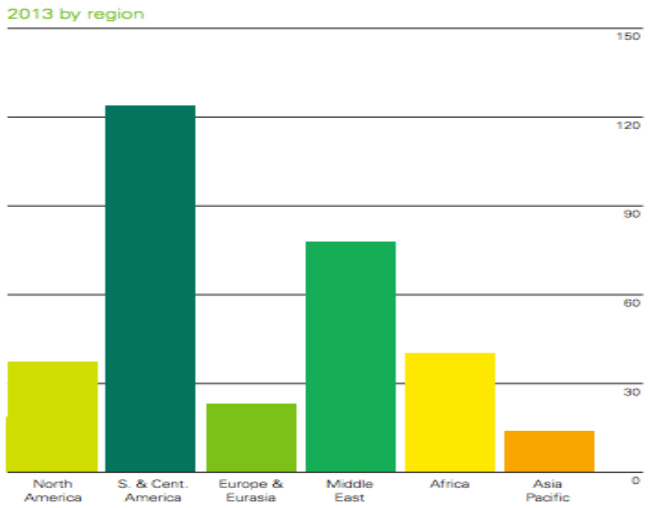

Figure 1 Reserves-to-Production (R/P) Ratio (BP; 2014)

The result of our energy dependence in this country continually resurfaces in the form of oil prices. The recent decision by O.P.E.C. to maintain supply levels, causing fluctuations in the oil market, gives cause for the U.S. and other countries to further seek energy independence. The price volatility of oil over the past 150 years can be seen in direct correlation with significant world events, shown in Figure 1.2. This contributes further to the notion that energy independence should be sought by the US and other oil dependent economies. In the US, a dependence on imported fossil fuel could be mitigated through the development of a sustainable source of biofuels.

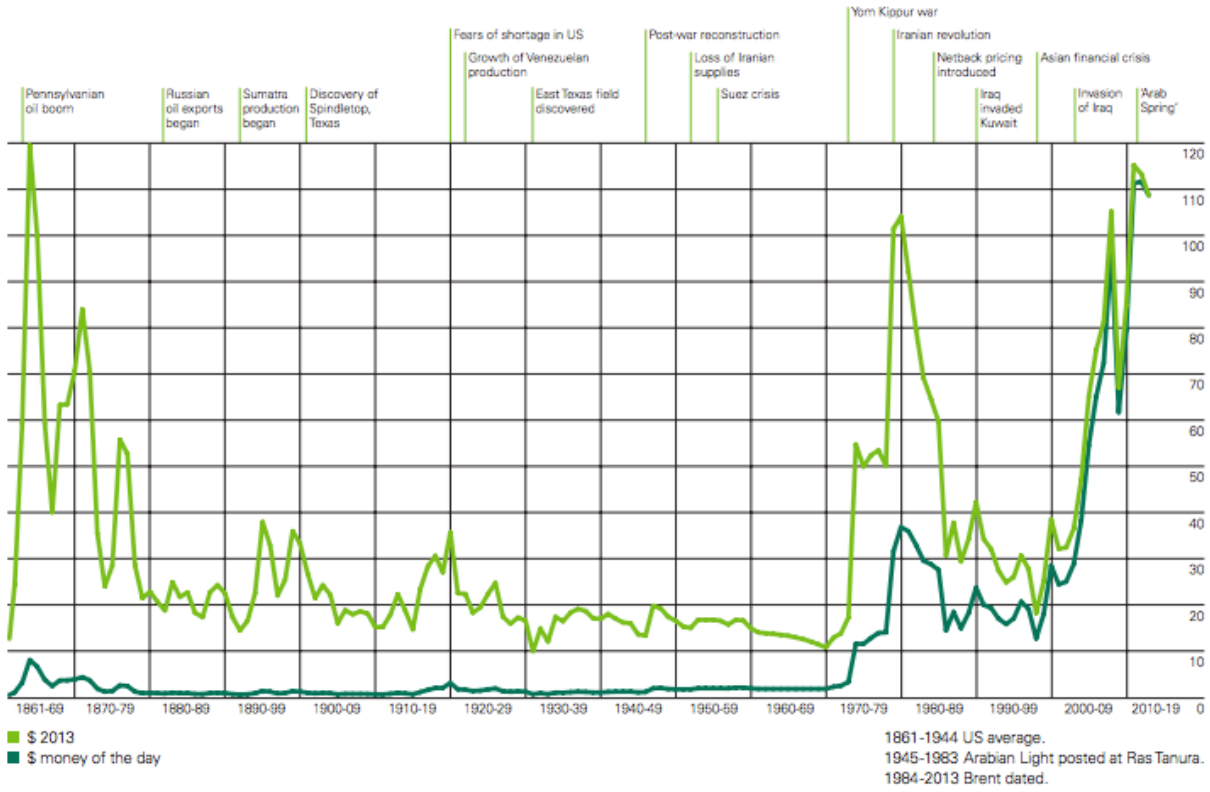

Figure 2 Reserves-to-Production (R/P) Ratio (BP; 2014)

1.2 Renewable Resources

Renewable resources offer an alternative to fossil fuels. Biofuels, hydroelectric, solar, wind, geothermal, and carbon sequestration are at the main forms of renewable energy that are being explored today (*Mata et al. 2010*). The first and most obvious approach to choosing a biofuel is the availability followed by the potential for use. The transportation industry is mainly calibrated to the utilization of liquid fuels. Biofuel crops can be readily grown and harvested and can provide a viable alternative to liquid fossil fuels. First generation biofuels are primarily derived from arable land crops such as sugarcane, sorghum, wheat, rapeseed, corn and maize as well as other vegetable oils or fats.

These biofuels can be broken down into two main groups; bioethanol and biodiesel, which can categorically replace transportation fuels entirely. Bioethanol comprises mainly of

ethanol, which lies in the ethyl group (C_2H_5OH) also known as ethyl alcohol. The ethanol is produced by sugars derived from plant-based crops. It can be produced to replace gasoline as a high-octane fuel. Vegetable oils or other forms of fats can produce Biodiesel. Thermochemical conversion of the lipid will yield fatty acid esters (FAEs). The biodiesel can then be used in mixtures with hydrocarbon based diesel, in varying amounts, to power diesel equipment.

1.3 Algal Energy

Algae and algal research has gained increasing attention because of its versatility. This naturally occurring, biologically robust organism can be grown in a variety of conditions. Combine this with its multiple and often parallel uses, in the form of a biofuel source and a GHG mitigation in growth, the argument for algae then requires further investigation. Algae falls under the classification of third generation biofuels, which is the use of non-food feedstocks to produce biofuels. This classification forms an important distinction in the use of biofuels. First generation biofuels consist partially of human food sources and must then compete for arable land, contributing to food supply and water shortages. Second generation biofuels consist mainly of lignocellulosic agriculture and forest residues, however this also raises questions over arable land competition for crop production. Algae then falls under the category of third generation biofuels, which is thought to address those issues pertaining to first and second generation biofuels (*L. Brennan, P. Owende 2010*).

It is well studied that algae provides and efficient biological sequestration of CO2 (*Mata et al. 2010, Brennan et al. 2010, Das et al. 2012*). Algae have been evaluated at their ability to reduce emissions in flue gasses. *Zeiler et al. 1995* studied the effect that flue gasses had on biomass productivity, ultimately reporting favorable results. The carbon dioxide released at combustion should be equal to the CO2 fixation that occurs at the growth stage of the algae

(*Mata et al. 2010*). The CO2 fixation of algae through photosynthesis has a potential to considerably reduce carbon emission and can be implemented on a variety of emission producing process.

Chapter 2

Algae as a Biofuel Feedstock

Algae has been heavily researched both as a source of food and as a potential feedstock for sustainable fuel production. In the mid 1970's, Eastern Europe saw the use of open-pond algae systems to commercially grow algae as a food source (*Ugwu et al 2008*). Later, the United States attempted algal growth in open ponds for water treatment. The many attempts to utilize algae in various forms has fueled its research; from biosorption of heavy metals and chemical production, to CO2 fixation and biofuel production. The attraction to algae as a source for biofuel stems from its ability to multiply quickly, its year round growth, efficient carbon fixation, and lipid productivity. Microalgae is more largely a feedstock for bioenergy; including bioethanol, biodiesel, jetfuel, and many other forms of liquid energy.

The process of algal biomass conversion to biofuel involves five basic steps, all requiring energy input, is displayed in Figure ##. The growth and cultivation stage involves all of the inputs required for photoautotrophic cultivation (e.g. light, CO2, and nutrients). Harvest generally involves a significant input via mechanical or thermal energy to dewater the algal crop. Cell lysis and extraction of intracellular matter can be achieved by either chemical or mechanical means. Thermochemical biomass conversion then yields useable biofuel.

Figure 3 Diagram of Biofuel production process

2.1 Algae

Microalgae are a simple yet very efficient microorganism. Their lack of complex plant structure (eg. Roots, stems, leaves) allows them to focus on rapid growth of the cell, including useful lipids. Microalgae are considered Eukaryotic cells, meaning they carry intra-cellularly, organelles required to survive and reproduce (*Brennan and Owende 2010*). Algae can be photoautotrophic or heterotrophic. Photoautotrophic algae require only CO2, light and nutrients to survive, whereas heterotrophic algae require the addition of organic compounds and nutrients. The use of light and CO2, both abundantly available, make photoautotrophic algae the obvious choice for research in the sustainable field. This also makes it the only economically reasonable method for mass production.

2.2 Mechanisms for Growth

Algal growth is determined primarily by three factors: light availability, nutrient availability, and carbon dioxide. Algae can be grown on a large scale using one of two common cultivation techniques; open pond systems or closed cultivation systems. Open pond systems use large artificial ponds and raceways to contain a large amount of algal biomass, often entirely exposed to open air. Raceways are long open channel containers in which a large paddle wheel circulates the water and creates a flow direction. They are used for mass cultivation and can utilize free natural resources such as sunlight to assist in algal growth. Open raceways, in comparison to closed systems, are cheap to build and maintain and do not require a large energy input. However, as research has been done on algae strains to yield higher production, some of the high yield algae is not suited to an open environment. In an open pond reactor, contamination is difficult to avoid and the local species of algae along with other micro

contaminants commonly prevails easily over the monoculture of desired algae. Other factors such as evaporation losses and light limitation make open pond systems difficult to justify at this stage.

Closed photobioreactors most commonly employ the use of clear tubes, vertically or horizontally stacked, to hold the algae. These systems have a much higher initial cost as well as an overall higher operational cost, however they are able to functionally isolate a monoculture of algae. This allows for the use of bio-engineered strains of algae to be implemented and utilized as a viable source of biofuel. Autotrophic cultivation requires reasonable control over the system as a whole. The closed system allows for precise control over all growth and cultivation parameters including light, temperature, pH, agitation, and CO2 inputs.

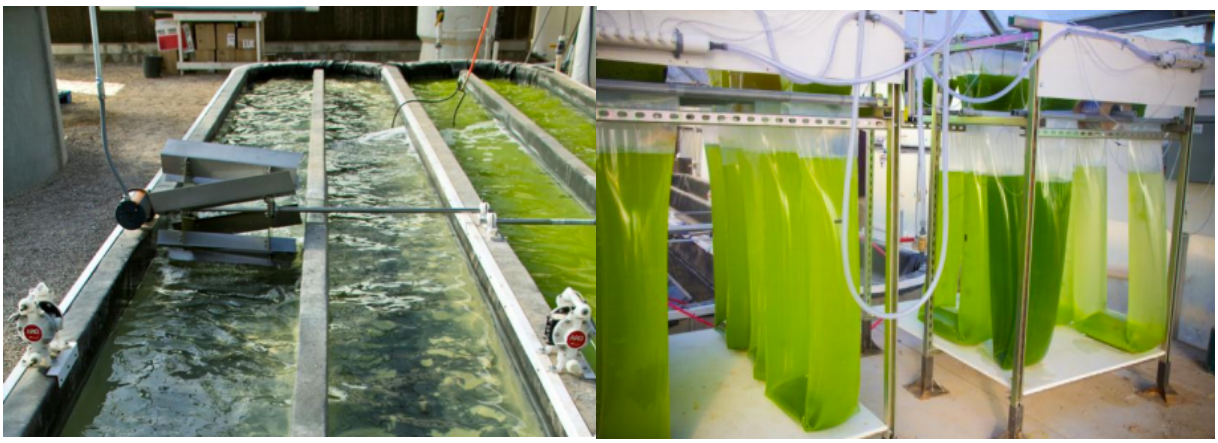

Figure 4 NMUS's Open Pond Reactor (left); NMSU's Closed Photobioreactor (right)

Closed photobioreactors (PBR) are widely accepted as being more efficient than open systems in terms of biomass productivity (*Brennan & Owende 2009, Ugwu et al. 2007, Shih-Hsin Ho et al. 2010*).

A small, lab-scale photobioreactor system was constructed for growth of two algal strains. 500ml volumetric flasks were used to contain the algae and low-flow aquatic air pumps were used to circulate air through the liquid medium. A grow tent and fluorescent grow-light were used to control the amount of light provided for algal growth. The light was set on a timer to optimize photosynthetic efficiency of the algal strain. *Rastegary 2013* reported a light/dark cycle of 16:8 as achieving the highest biomass increase in a lab setting. A bio-mass measurement was taken to ensure that results achieve in the lab were comparable to those reported in literature.

2.3 Biomass Harvest and Extraction Techniques

The first step in the process of extracting biomass requires that the algae be de-watered and concentrated, known as harvest. Given the current biomass extraction techniques, this is a required step in achieving the highest lipid yield. The energy input required to dewater algae on a production scale is cost prohibitive.

There are three processes by which algae can be separated from water; centrifugation, filtration, and sedimentation. Centrifugation, at a large scale, has a very high initial cost as well as large operational costs. Similarly, filtration has a high initial cost with routine maintenance costs inherent to the system. Sedimentation requires the least energy inputs to achieve suitable concentration. When stagnant, algae can settle out of the growth medium at a rate of up to 1mm/s (*Posthuma 2009*). Flocculation is another alternative whereby a flocculent is added, clumping the algae together. However, this requires the input of a flocculent as well as additional processing to separate the algae. The process by which extraction is explored in this

thesis removes the harvest and concentration stage all together, greatly reducing the end cost by extracting the algae in wet form.

In order to adequately compare current extraction techniques with the method described in this manuscript, the current extraction methods must be examined. There are several methods currently used in the extraction of intracellular matter from algal feedstock. Mechanical, solvent, sonication, and microwave are among the most common methods used for cell lysis. Each method increases the cost of processing via energy input or addition of chemicals.

2.3.1 Mechanical Extraction

Mechanical extraction, like the majority of extraction techniques, requires high biomass concentrations prior to processing and, as discussed previously, requires an energy input that inevitably decreases the overall efficiency of the process. Mechanical extraction is often preferred however, due to its simplicity. Common mechanical extraction techniques include bead milling, pressing, high-pressure homogenization. These methods generally utilize mechanically applied high pressure which lyse's the cell, releasing the lipids. Bead milling involves the use of small beads packed into a vessel agitated by a rotating shaft. The high speed agitation of the media ruptures the cell wall. Bead milling is often combined with solvent extraction to increase the effectiveness. Mechanical pressing requires a dry algal biomass. Up to 30% of the final biofuel processing cost can be attributed to drying the algae for extraction (*Kumar et al. 2015*). Pressing is one of the oldest methods for oil removal from biomass. It achieves cell lysis by applying high amounts of pressure in a confined space. Finally, high-pressure homogenization imparts extremely high pressures on the concentrated but wet algal stream, forcing it through a small space. This can produce sharp pressure changes as well as

high shear, resulting in cell disruption. *Mercer & Armenta 2011* report mechanical disruption techniques achieving of up to 20.5% oil recovery.

2.3.2 Solvent Extraction

Organic solvents are frequently used in downstream processing of algae to degrade cell walls. Oil has a high solubility in organic solvents making this method of extraction more desirable and more efficient. Solvent extraction using benzene, acetone, hexane, and various other solvents is a commonly used and reported practice in intracellular biomass extraction. *Mercer 2011* reports hexane extraction at over 25%. The Bligh and Dyer method (*Bligh & Dyer 1959*) is a commonly used extraction technique for lipids. It consists of multi-stage chemical extraction consisting of chloroform and methanol.

Mechanical extraction can be combined with solvent extraction to increase the amount of oil extracted. The use of two methods simultaneously greatly increases the energy inputs to the system, thereby reducing overall efficiency. This method also carries the drawback of solvent recovery after the extraction process. It is difficult and energy intensive to recover all of the solvent used so the final product is often contaminated with solvent.

2.3.3 Sonication Extraction

Sonication extraction has recently been reported in literature as a viable method of fully wet lipid extraction. Ultrasound as well as audible range techniques have been explored as methods of lipid extraction (*Gogate et al. 2001, Rodriguez 2012*). Common techniques in sonication include the use of submerged ultrasonic probe systems, known as horns. The Dakshin bath is an efficient method of cell disruption in which a reservoir containing the reactions solution is connected to trasducers, inciting cavitation. *Gogate et al 2001* reports efficiencies as

high as 38% for the Dakshin bath. Scalability of the system is difficult due to the complexity of the system set up.

2.3.4 Hydrodynamic Cavitation Extraction

Hydrodynamic cavitation extraction of intracellular matter is scarcely reported in literature. *Balasundaram and Pandit 2001* compare the rate of yeast cell disruption of hydrodynamic cavitation against sonication and high-pressure homogenization, ultimately reporting cell disruption of hydrodynamic cavitation an order of magnitude higher than the other methods. This method utilizes an orifice plate placed in a pressurized line to disrupt flow. The plate causes a large pressure drop in the fluid, giving rise to cavitation where cell disruption is achieved. This work explores the effects of certain functional parameters on the efficiency of hydrodynamic cavitation.

Chapter 3

Cavitation

Cavitation is defined as the formation and existence of cavities in a homogenous liquid medium. This can be achieved several ways: adequate tension in the liquid or a local energy deposit on the fluid. *Shah et al. 1999* describes the four basic methods that exist under these classifications, as seen listed below:

-Hydrodynamic/Hydraulic Cavitation (velocity variations in fluid stream)

-Acoustic Cavitation (pressure fluctuations introduced to liquid)

-Optic cavitation (high intensity light/laser)

-Particle Cavitation (high intensity light or by elementary particle disruption in the liquid)

Listed above are methods that can be used to incite cavitation in a fluid medium. At inception, the bubbles can originate from already present cavities that are subsequently expanded or from the formation of bubbles due to an adequate pressure gradient or oscillation. There are several methods to induce cavitation mechanically by work input to the fluid. Acoustic and hydrodynamic cavitation occur when sufficient tension is introduced to the fluid. The driving force for acoustic cavitation involves fine tuning oscillatory vibrations through the liquid to achieve cavitation. Hydraulic, or hydrodynamic cavitation is achieved through a large pressure drop created in a steady flowing system. Several studies have shown that hydrodynamic cavitation can achieve significantly increased efficiencies over acoustic cavitation (*Mohlkar et al. 1999, Gogate et al. 2004, Pandit et al. 2001*). An overview of the categories of cavitation is seen in Figure 3.1 as described by *Lauterborn, 1980*.

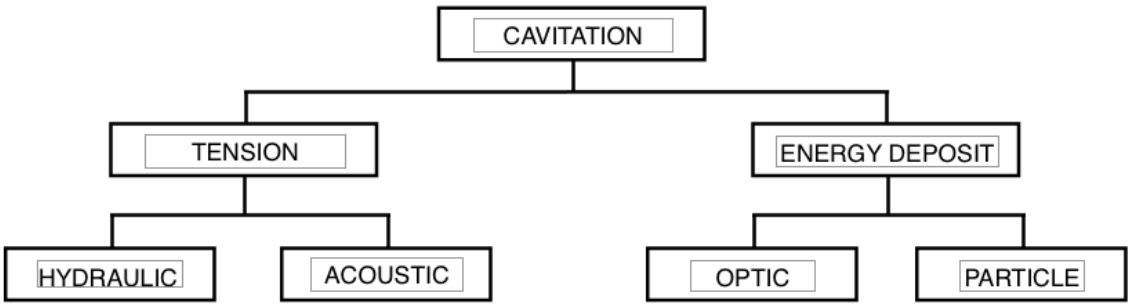

Figure 5 Classification scheme for the different kinds of cavitation (Lauterborn, 1980)

3.1 Two Phase Flow

It should be noted that boiling and cavitation are similar yet achieved differently. Figure 3.2 (left) shows the phase diagram for water. Here, the line connecting the triple point, Tr, and critical point, C, represents the boundary between the liquid and vapor regions. Boiling is achieved when heat is added at constant pressure, causing the liquid temperature to rise above the saturation temperature. Cavitation, in the opposite sense, is caused by a loss in liquid pressure to the extent that the vapor pressure threshold is surpassed for the fluid medium at constant temperature. The bulk temperature of the fluid should be kept as low as possible because of the dependence of cavitation on saturation temperature. *Shah, 1999* argues that at a higher liquid temperature, cavitational yields will decrease as the cavity bubble would fill with vapor of the liquid, thereby causing the bubble collapse to be "cushioned" and therefore producing lower pressures and temperatures.

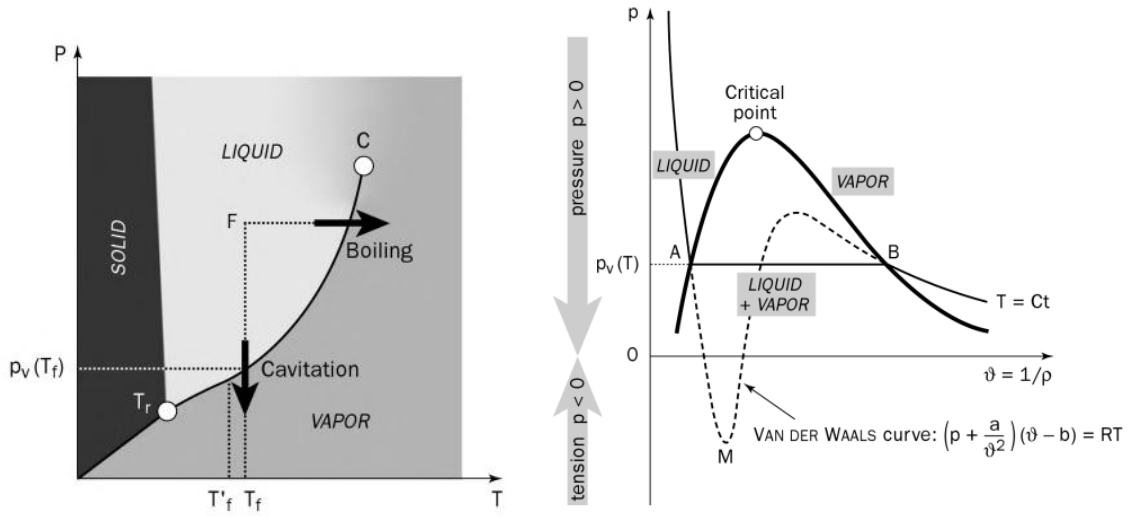

Figure 6 Phase diagram of cavitation (left), Andrews-isotherms (right) (Franc el al 2004)

Cavities form via a nucleation sites in the fluid. These imperfections offer a locale of decreased fluid tensile strength, inciting cavitation. Three main steps exist in the formation of a cavity bubble; breakdown of the liquid, filling of the void with vapor, vapor saturation. *Franc 2004*, theorizes that these three steps in void creation occur almost instantaneously. When devoid of imperfections, the liquid may follow the curve AMB, in Figure 3.4 (right). This curve, known as the Andrews isotherm, can be approximated by a modification to the ideal gas law via the Van Der Waals equation of state. As previously stated, this requires that the liquid have no impurities. Here, the pure liquid can actually undergo tension without a phase change on the order of about 1000 atmospheres. Real world, engineering applications however require imperfections in the liquid to be considered. These imperfections allow the liquid to more closely approximate curve AB.

3.2 Physical Effects of Cavitation

3.2.1 Cavitation Through a Single-Orifice

Cavitation through a single hole is the simplest form of orifice plate cavitation. Using this example, the inception of the cavitating condition is explored. Orifice plate cavitating flows occur at high Reynolds numbers placing the flow in the turbulent regime. Control over the physical parameters to achieve the desired cavitational intensity then is necessary. The flow at the inlet of the orifice is set to a pressure, P1. This pressure will, depending on the orifice plate geometry, increase the velocity at the expense of the pressure head. As the cross-sectional area of the flow is reduced, the minimum pressure will occur at the point of vena contracta. This point lies just downstream of the orifice as seen in Figure 3.3.

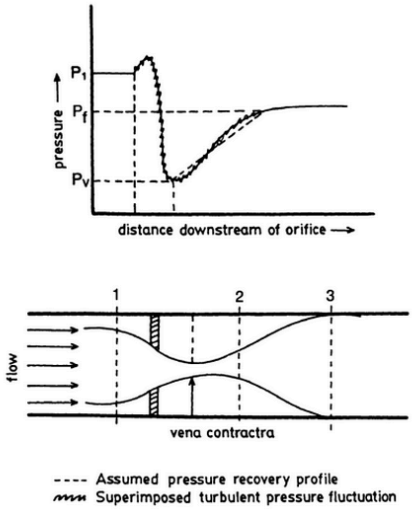

Figure 7 Typical pressure distribution across an orifice plate in pipe flow, Moholkar et al. 1999

When the pressure at the vena contracta falls below the vapor pressure of the fluid medium, cavities are formed. The cavities typically incite at nucleation sites due to impurities in the liquid. This occurs at the shear boundary layer, which is the interface

between the high-velocity flow and the downstream turbulent zone. The cavities are carried down stream and collapse violently as the pressure recovers.

3.2.2 Bubble Dynamics

At this point, is necessary to examine the behavior of a single cavity. There are several assumptions that need to be made when considering a single cavity; First, since the cavitating flow is caused by the shear layer of the liquid beyond the point of vena contracta, the cavities can be assumed to have a spherical geometry throughout their life. The life of the bubble can be described in three stages; inception, growth and collapse. In cavitation, it is well accepted that at inception stage of bubble growth can be assumed to be isothermal, where the bubble exchanges heat with the surrounding fluid to maintain constant temperature. *Shah et al. 1999* describes the wall movement of a spherical bubble:

$$\frac{dr}{dt} = \frac{R^2(\frac{dR}{dt})}{r^2}$$

where R is the radius of the bubble wall, and dR/dt is the velocity of the wall. Then dr/dt is the radial velocity in the liquid space at time t. This consideration only holds for bubble radii larger than zero.

Examination of an empty cavity can be seen by the Rayleigh-Plesset equation, below:

$$\left[\frac{p_B(t) - p_\infty(t)}{\rho} = R\ddot{R} + \frac{3}{2}(\dot{R})^2\right] + \frac{4\mu}{\rho}\dot{R} + \frac{2\sigma}{\rho R}$$

The term on the left represents the pressure effect, where Pb is the pressure in the bubble and P_∞ is the far field pressure as related to the bubble. The first two terms on the right hand side of the equation consider the inertial effect of the single cavity and ρ is the density of the fluid. The terms within the brackets represent the basic bubble dynamics equation. Outside the bracket, viscous (μ) and surface tension (σ) are considered.

A further assumption in the formation of a bubble includes incompressibility of the medium and adiabatic collapse of the bubble, thus neglecting heat and mass transfer across the bubble wall. The adiabatic collapse, which happens at a much shorter time interval than the growth, gives rise to relatively large temperatures and pressures. Fujikawa and Akamatsu 1980 reported extreme temperature and pressures associated with cavitation. This extreme environment, although its existence is on the order of a fraction of a microsecond, is generally accepted as the driving factor to cavitation chemistry.

The velocity and pressure profiles were obtained using FLUENT for a single orifice reactor, is displayed in Figures 3.4 and 3.5. The turbulence contour is given in the Appendix. The single-orifice model assumes steady state, 2-D, axis-symmetry flow and is modeled at the same geometry of the reactor used in the study.

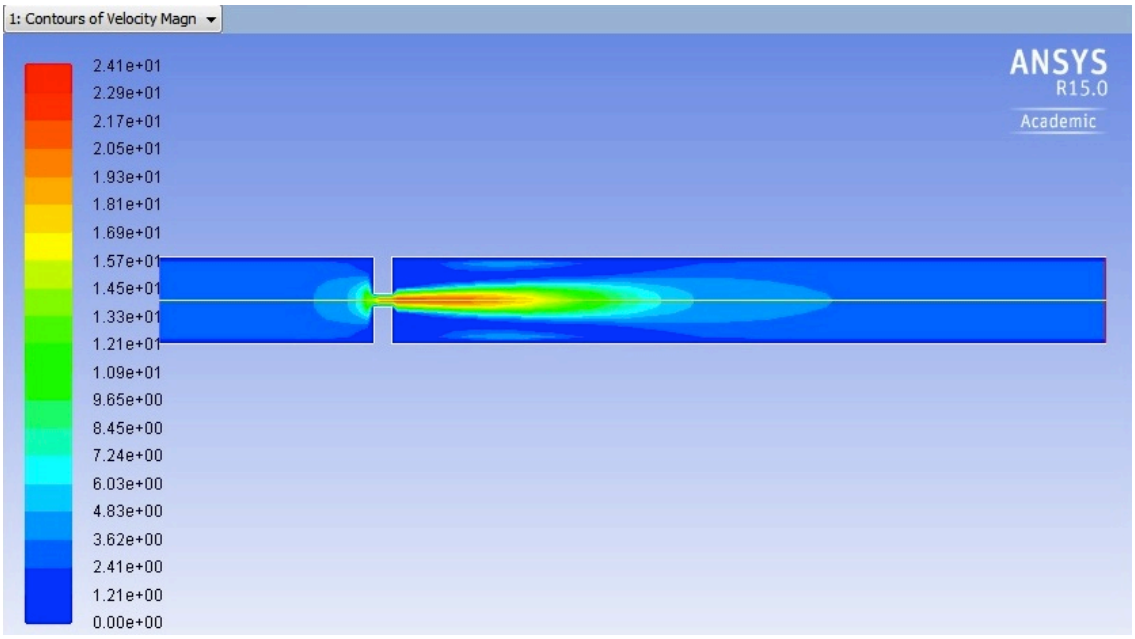

Figure 8 Velocity Contour for single orifice cavitation

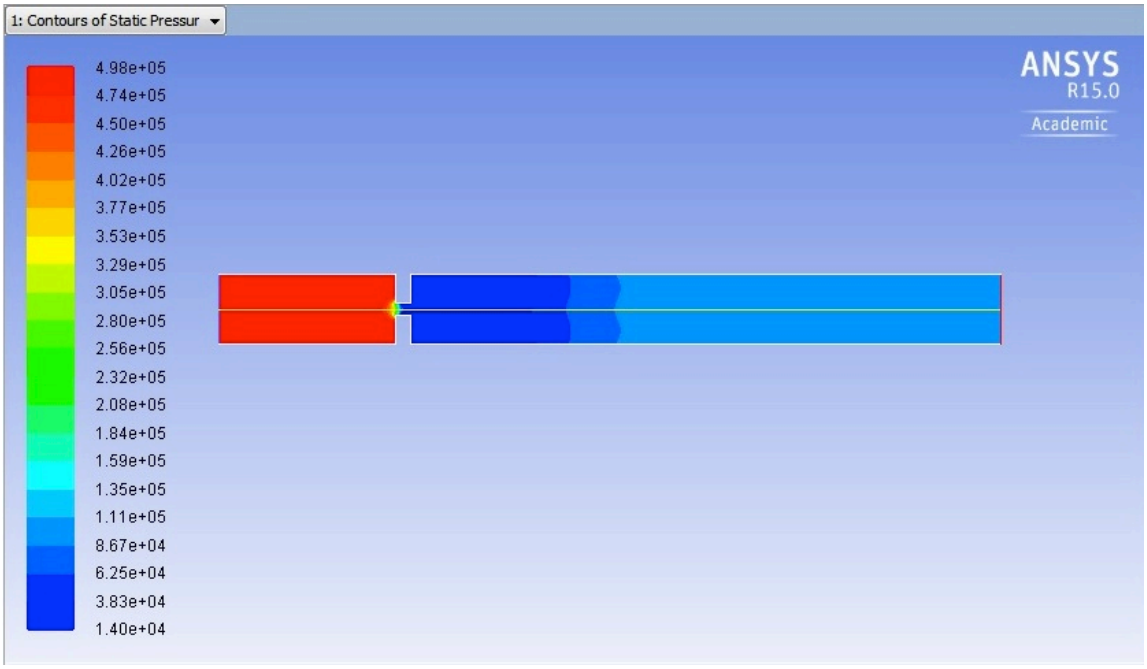

Figure 9 Pressure Contour

3.3 Parameters

High flow rates and fluid velocities, as seen in the system, suggest little difference in static and stagnation pressure indicating a flat axial velocity profile. *Kumar et al. 2000* reported the variation of Δh against the radial distance to be less than 5% by traversing a pitot tube radially through the flow. Thus, fluid flow across an orifice plate can carry this assumption. In the design of the orifice plate symmetry should be considered critical to obtain results reflecting the design.

3.3.1 Cavitation Number

The cavitation number is a parameter used for the prediction of cavitation. Cavitation number is a dimensionless parameter

$$\sigma_C = \frac{P_f - P_v}{\frac{1}{2}\rho U^2}$$

Here, P_f is the downstream pressure, which will be used interchangeably with P_2 throughout this work, P_v is the vapor pressure of the fluid, ρ is the density of the fluid medium, and U is the velocity of the fluid through the orifice(s). Generally speaking, this parameter is the fluid tension, Pf-Pv, created by the pressure drop, over the free-stream dynamic pressure

Yan et al

The free area parameter, β, is a useful and well established orifice plate design parameter

$$\beta = \frac{Free\ Area\ of\ Holes}{Flow\ Area\ of\ Pipe} == \frac{N*\frac{\pi}{4}d^2}{\frac{\pi}{4}*D^2}$$

which can simplify to

$$= \frac{N * d^2}{D^2}$$

where N is the number of holes in the orifice plate, d is the diameter of the orifice(s) and D is the diameter of the main line.

$$\alpha_s = \frac{Total\ Perimeter\ of\ the\ Holes}{Total\ Flow\ Area\ of\ the\ Holes}$$

$$\alpha_s = \frac{\pi d}{\frac{\pi}{4} d^2}$$

Here d is the diameter of the orifice used.

3.3.2 Spreading Ratio in the Downstream Liquid Jet

The cavitating liquid jet, beyond the point of vena contracta will spread in a radial manner until it reaches the pipe wall. *Yan & Thorpe 1990* defined this spreading ratio for a liquid jet as

$$\alpha' = \frac{d_x - d_v}{2x}$$

where dx is the liquid jet at distance x from the orifice and dv is the diameter of the liquid jet at the point of vena contracta. In the design of the orifice plate it is necessary to space the orifices according to the downstream behavior. In order to create an unobstructed liquid shear-zone leading to more predictable cavitation, the orifices should be spaced accordingly. This also lends to the efficient distribution of the cavitation downstream of the vena contracta of the multiple-hole orifice plate. The downstream turbulence will also contribute significantly to the distribution cavitating flow. Setting a control free area ratio and moving the orifices out radially may reveal a difference in cavitation distribution. This distribution may aid in driving cavitation

reactions more efficiently in the bulk medium, requiring less time for the desired output, in this case, cell lysis.

3.3.3 Proposed Shear Parameter

Due to differences in size and volumes across the field of research in hydrodynamic cavitation a new parameter was created to aid in the design process of a hydrodynamic cavitation setup. The parameter relates the shear perimeter of the sum of the orifices to the area downstream of the plate in the reactor. The parameter utilizes a combination of previous parameters, α_s and β, to aid in the design of multiple-hole orifice plates. The new parameter is designated as lambda, λ_S (lambda-shear), shown below:

$$\lambda_S = \frac{\alpha_s}{1/\beta}$$

$$= \frac{\frac{\pi d}{\frac{\pi}{4}d^2}}{1 \Big/ \frac{N * \frac{\pi}{4}d^2}{\frac{\pi}{4} * D^2}} = \frac{N\pi d}{\frac{\pi}{4}D^2}$$

Simplified to read,

$$\lambda_S = \frac{4Nd}{D^2}$$

Where d is the orifice diameter, N is the number of orifices and D is the area downstream of the orifice plate. Lambda-shear relates the total perimeter of the orifice holes (shear perimeter) to the downstream area. As discussed earlier, the shear perimeter is the perimeter of the orifices on the plate that produce fluid shear downstream of the plate. It is necessary to

correlate this to the pipe diameter in order to aid in effective design of a reactor with predictable yield.

3.4 Cavitation Chemistry

Cavitation has been widely reported to incite chemical change. Hydrodynamic cavitation has been compared and deemed similar to the sonochemical process, finding similar reaction temperatures induced by both acoustic and hydraulic forms of cavitation (Pandit et al. 2000). The increased dissociation rate of water brought about by the extreme environment in cavitation is given as follows.

$$H_2O \rightarrow H^+ + \quad OH^-$$

Here, increased dissociation rate of water can be attributed to the high mass transfer rates achieved in cavitation. These highly active hydroxyl radicals and other reactive species are then available to react with other species in the bulk medium. This short-lived extreme environment inside the aqueous solution, brought on by sufficient pressure drop in the system has been used to accelerate chemical reactions, including oxidation reactions and even trans-esterification reactions (Gogate et al. 2004).

3.5 Experimental Methods

The use of cavitation for a method of cell disruption is relatively new. A standardized method for quantifying hydrodynamic cavitation as a driver for chemical reactions is lacking in literature. The flow conditions however, can readily be adjusted; especially in a closed hydraulic system. Here, control over the physical parameters allows the designer of the system to control different variables to achieve desired output. Size, power, flow rate, temperature, and orifice geometry are the main controlling factors of the system, which makes the hydrodynamic cavitation readily scalable.

3.5.1 Hydrodynamic Reactor

The design and construction of the hydrodynamic cavitation reactor saw several preliminary designs before an optimal reactor was constructed. The reactor consists of the entry and exit flanges, the viewing lens, supports, orifice plate, and O-rings as required to seal the device properly. The reactor entry and exit flanges, were constructed of 304 stainless steel and machined down to 8mm (0.3 in) thickness with an inner diameter of 19.05mm (0.75 in) to accommodate the stainless 316L sanitary ferrule fitting (L14AM7-R75 Dixon Sanitary), which was TIG welded into place. The ferrule fitting was chosen so that the orifice plate in-line on the reactor could be removed and replaced in order to easily test a variety of orifice plates. The ferrule fitting had an inner diameter of 13.5mm, considered throughout the work as the upstream diameter of the reactor. Three (3) six inch, stainless steel rods were used to support the viewing lens, attached to the plate via screws. The viewing lens, in the cavitation zone downstream of the orifice plate, 0.159m (6.25 in) plexiglass tube of inner diameter 15.90mm (0.626 in) which is considered the downstream diameter in the reactor seen in Figure ## below. The system was

designed to operate with pressures of over 700 psi, limited by the clear PVC tubing used to feed the system.

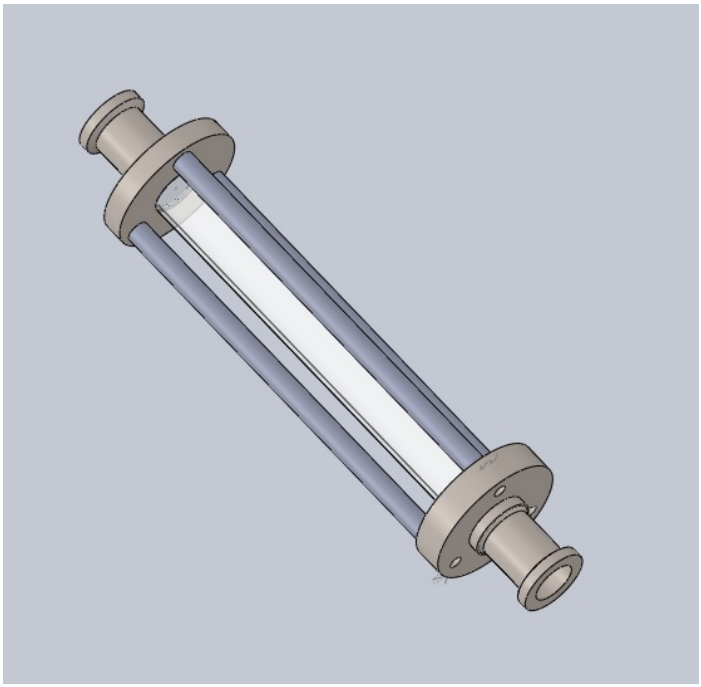

Figure 10 Hydrodynamic Cavitation Reactor

3.5.2 Orifice Plate

Many iterations of the orifice plate were fabricated and tested throughout the project. The orifice plates were standardized at 2.6mm (0.1in) thickness and 19.05mm (0.75in) diameter. All of the considerations as described earlier in section 3.3 were utilized in the design of orifice plates. Preliminarily, 304-stainless steel was used but after losing several 1mm and smaller drill bits to the work hardening of the metal, it was deemed more appropriate to use mild steel. However, the use of steel introduced rust (ferric oxide) that was thought to affect the KI reaction as described in **4.4.4** of this work. Due to the adverse effects of the rust on driving the chemical reaction, 303 stainless plates were implemented. A cross-sectional view of a single orifice plate is shown below.

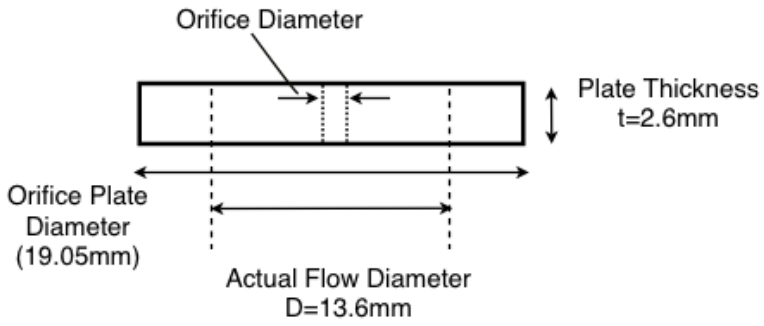

Figure 11 Orifice Plate Geometry

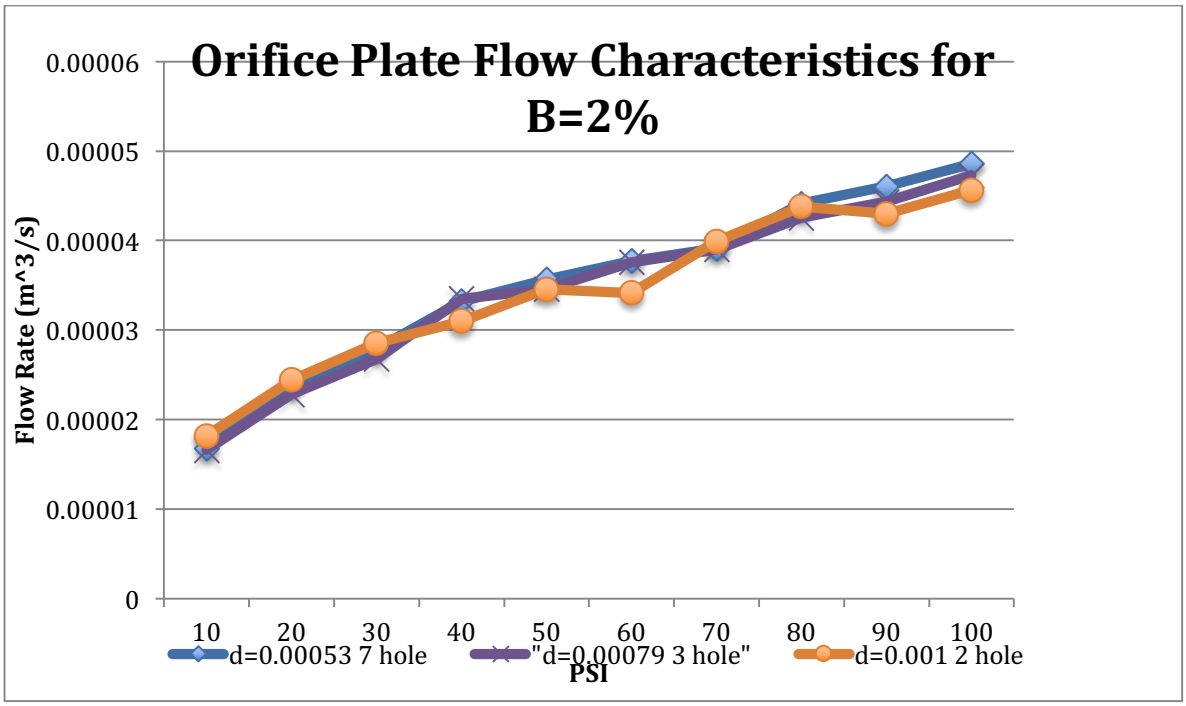

Figure 12 Orifice Plate Flow Characteristics

3.5.3 Motor Control and Pump Selection

A fluid pump capable of the volume flow requirements to incite cavitation in the system was selected. The pump used (L26475 Micropump Inc. Vancouver, WA) is a cavity style, magnetic drive gear pump consisting of helical gears (3.48 ml/rev), with a maximum flow rate of 12 L/min and a maximum differential pressure of 100 psi.

The flow rate of the pump was matched to an appropriate motor. The pump was coupled to a 5hp, 3-phase, electric motor (Baldor EM3212T) via a pump adaptor, pictured in **Figure##**, capable of 3450 R.P.M. The pump adaptor is a round aluminum plate, 0.5in by 6.62in, with an internal lip to center on the motor-shaft and 0.25in holes for attachment to the motor. The output shaft of the motor had to be removed and machined down to accept the ferrite coupling of the magnetic drive.

Accurate control of the motor required a 3-phase, 4KW Variable Frequency Drive (HY04D023B, Y&F Group Ltd. Hong Kong). The VFD employed a frequency range of 0.5-400 Hz. In order to maintain constant torque and maximum efficiency on the motor through the operating range a scalar control was applied to the motor, maintaining a fixed voltage to frequency ratio of 3.83. Upon operation with the cavitation reactor, an extended ramp time of 20s was implemented so that internal bubbles and air pockets could be eliminated so that the system could reach a steady state without first inciting chemical reaction through cavitation.

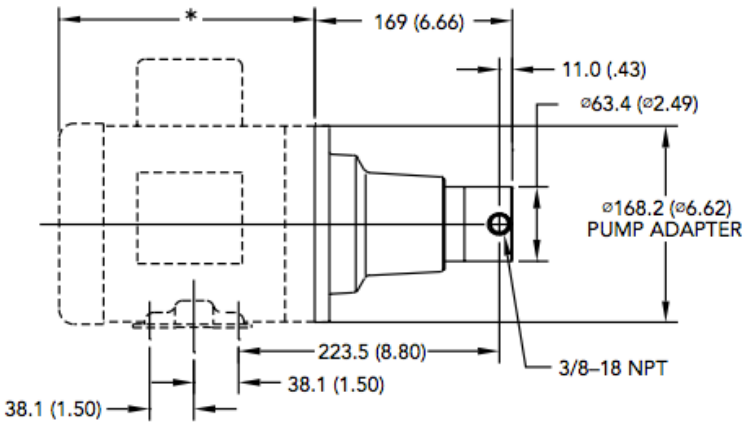

Figure 13 Schematic of Motor-Pump Setup (MicroPump GD)

3.5.4 Reactor System

There is one line (one direction) of flow in the system. The lines are 3/8" clear poly tubing and attached by hose-barb and line clamp. The solution starts in a 2000mL flask. Water or chemical solution is drawn through the line by the magnetic-drive pump. A pressure gauge is placed downstream of the pump, to monitor pressure before the orifice plate reactor. Since an accurate power control was implemented on the pump, no upstream valves were needed to regulate the upstream pressure. Downstream of the orifice is another pressure gauge to monitor the downstream condition of the flow. Beyond this, a valve was placed in line so that the downstream pressure of the flow could be controlled. The line terminates into the original solution with the line placed below the surface of the liquid to minimize introduction of air bubbles to the system. Due to the power dissipated to the liquid, the solution container was kept at 35C +/-4C via a liquid bath. The cooling water had to be pumped out and replaced to avoid rise in solution temperature. A diagram of the setup is displayed in Figure ## below.

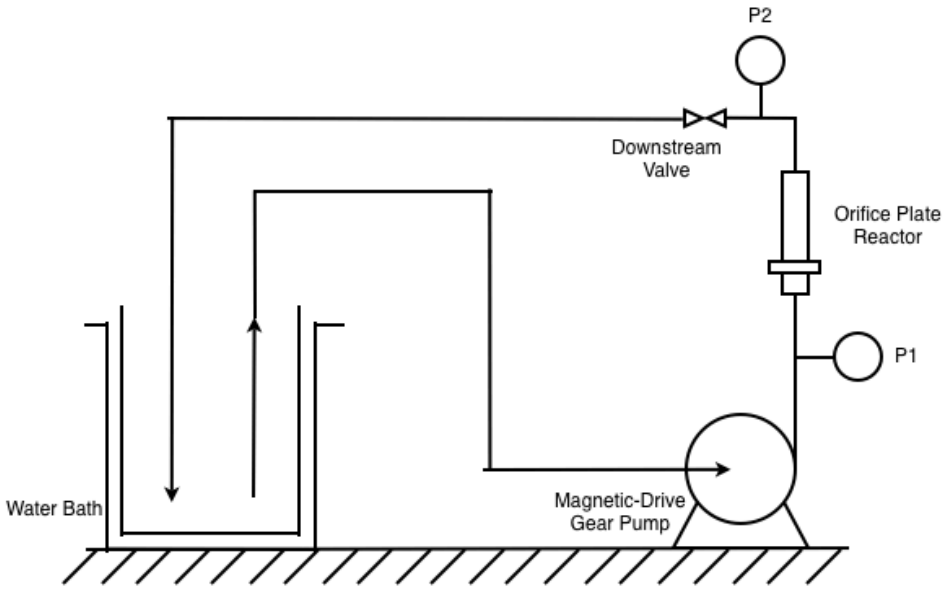

Figure 14 Physical Diagram, Orifice Plate Reactor

3.6.4 The Weissler Reaction

The Weissler reaction is generally accepted as the model reaction for quantification of cavitational intensity, where the cavitation event drives the chemical reaction in liberation of tri-iodide , I_3^-. This reaction is driven by the existence of the short-lived hydroxyl radicals via the formation and collapse of cavitation bubbles, as discussed in section 3.4 of this work. The Weissler reaction, in this experiment, consists of the decomposition of a 0.1M aqueous KI solution. The reaction pathway of the short-lived reactive species with the KI solution is shown below:

$$I + I^- \rightarrow I_2^-$$

$$2I_2^- \rightarrow I_2 + 2I^-$$

$$I_2 + I^- \rightarrow I_3^-$$

Potassium iodine, KI, was dissolved in deionized water to form a 0.1M/L solution, a commonly used molarity in verifying the cavitation reaction. The solution was prepared and stored in a non-reactive container, and used in 2L testing increments, per the size of the system. This 2L solution was introduced to the cavitating flow, at different pressures, equating to different cavitation numbers.

The tri-iodide ion seen in the reaction pathway above is then able to be analyzed spectrophotometrically via the addition of a starch solution. This solution is prepared by dissolving 1 gram of soluble starch with 100ml of distilled, deionized water. Samples were taken in 3mL increments over a reaction period of 20 minutes. When combined with the starch solution, the sample of aqueous KI becomes very slightly cloudy with the addition of each drop until no change can be detected. The samples were transferred into disposable plastic cuvettes and analyzed spectrophotometrically for absorbance at 355nm.

Chapter 4

Results and Discussion

4.1 Calculations

The calculations in this work are done so that the results reported in this text can be compared with those results of cavitation reactors from other bodies of work. The values of main importance to be extracted from this work are the flow parameters, cavitational yield and the system efficiency. In order to obtain the cavitational yield, the amount of liberated iodide from the KI solution must be quantified. The measure of cavitational yield is a generally accepted, standardized method of comparing cavitation across different types of cavitation devices.

When the starch is mixed with the KI solution in testing, the sample turns blue but not to the naked eye. To quantify this, the sample must be analyzed via UV/VIS spectrophotometer. The absorbance is measured over a specified distance, usually the width of the cuvette. The cuvette's used measured approximately 1 cm in length. Absorbance determined by the Beer Lambert Law and is given as

$$A = \varepsilon bc$$

Here, A is unit less and is known as the absorbance, ε is the molar absorptivity. ε is constant for the aqueous KI solution and is given in units of $\frac{L}{mol*cm}$. As mentioned above the absorbance is measured over a specified distance, given as b in the equation and "c" is the molarity concentration of the chemical solution.

4.2 KI Decomposition

Orifice plates at a free area ratio of 2% were tested via KI oxidation reaction. The desired cavitation number was achieved by controlling the upstream pressure of the system and thus the velocity of the fluid through orifice(s). Once an optimal cavitation number was established, the free area ratio was held constant and the shear parameter (λ_S) was varied, as discussed in section 3.3.3 of this work. Orifice plates with equal free areas with varied λ_S are shown in Figure##.

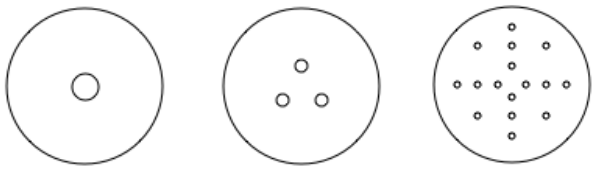

Figure 15 2% Free area, Varying geometry

The cavitation number, Cv, was varied on a specific plate in the aqueous KI solution. Different upstream pressures caused the cavitation number to change. Tests were run at 30 minute increments, with samples taken every 5 minutes. The results were analyzed spectrophotometrically.

The effect of the upstream pressure on the cavitation number is shown in Figure 16. The effect of cavitation number on the liberation of iodine as well as the iodine liberation rate vs. time are displayed below, in Figures 17 & 18;

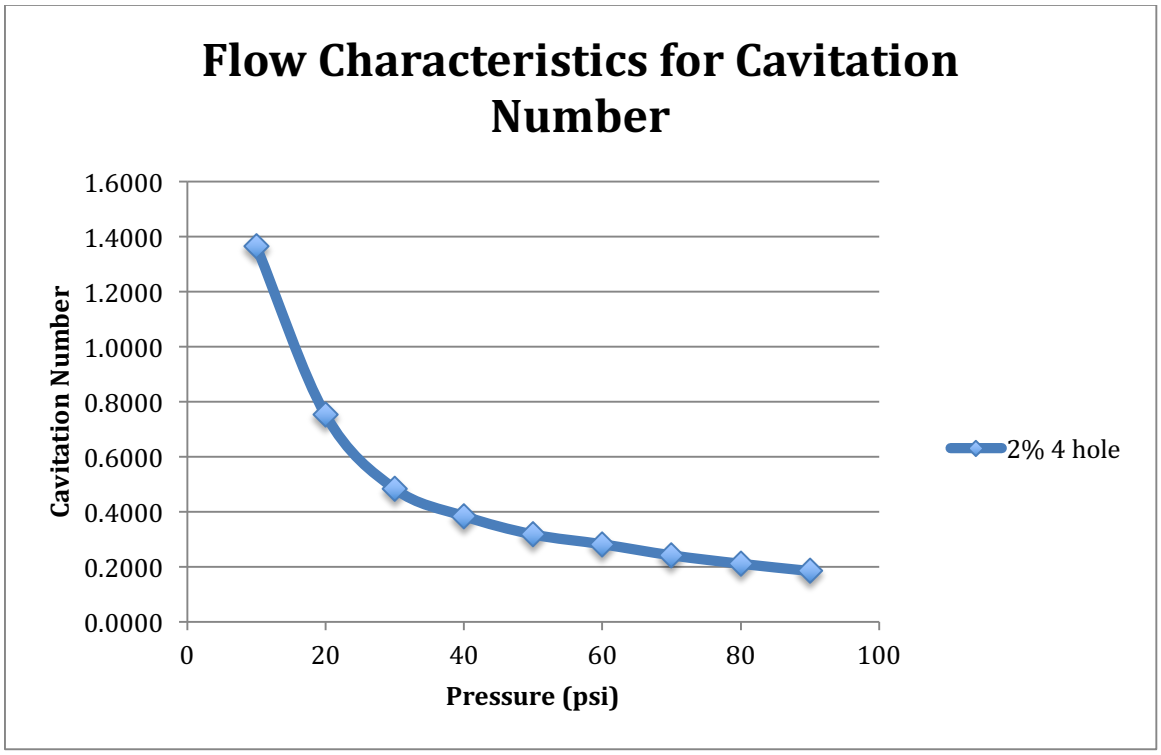

Figure 16 Pressure Effect on Cavitation Number

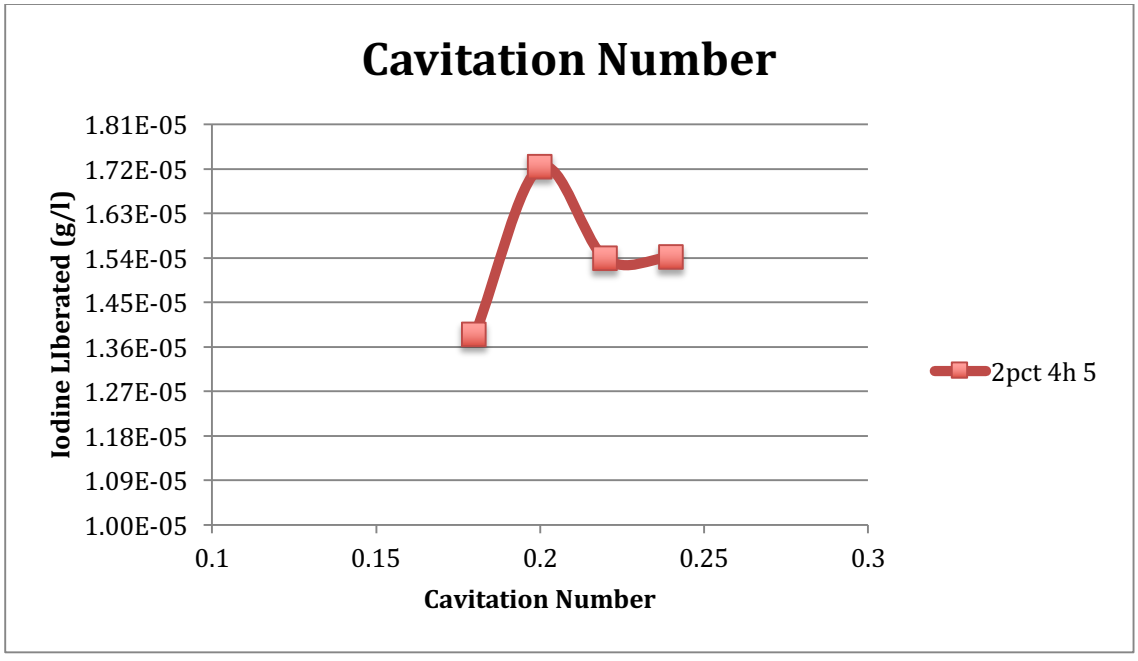

Figure 17 Cavitation Number vs. Iodine Liberated

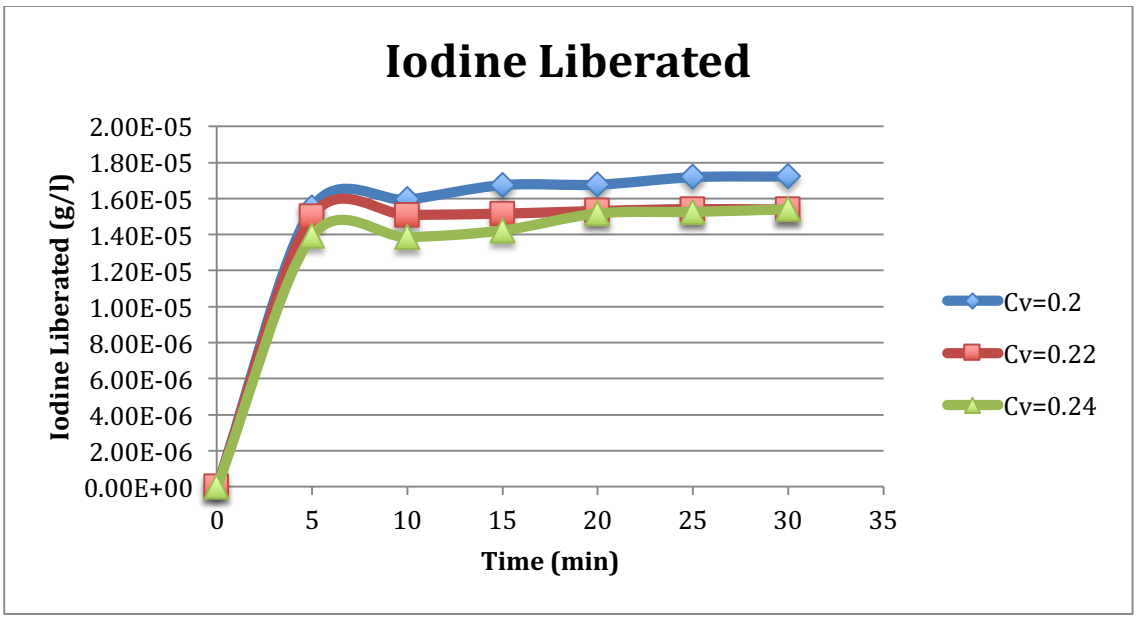

Figure 18 Cavitation Number vs. Iodine Liberated

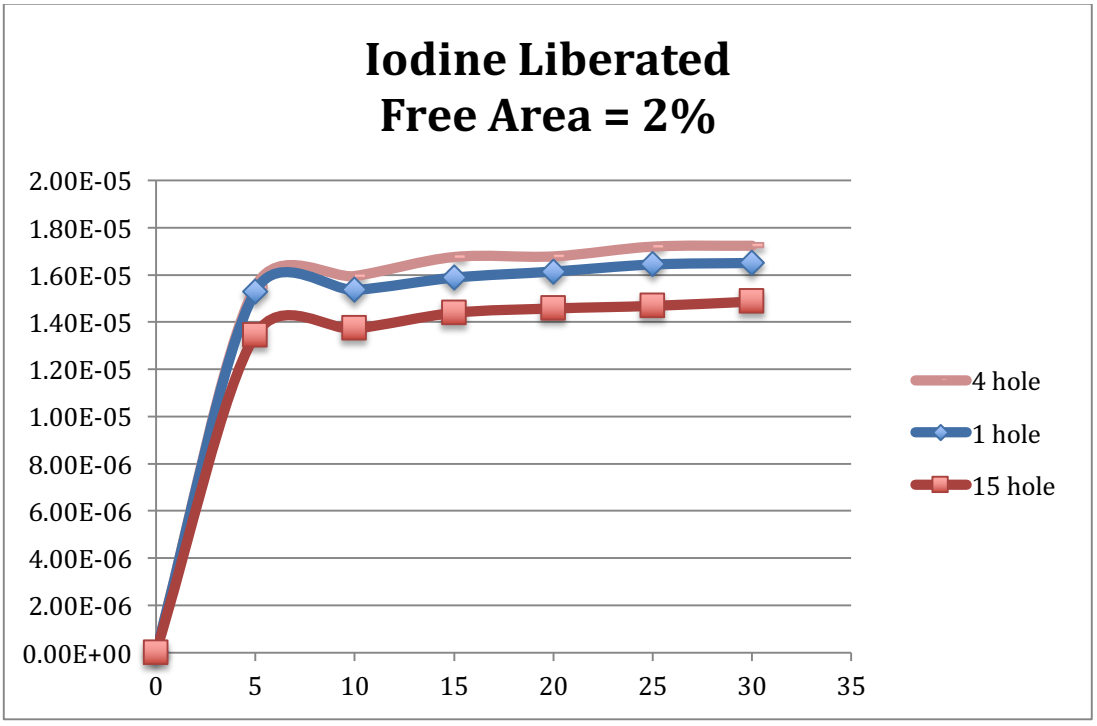

Figure 19 Iodine Liberated at 2% Free Area

4.3 Calorimetry and System Efficiency

When determining the amount of power done on the system, calorimetry is a commonly used and accurate approach. Calorimetry was performed on the insulated 2000mL system over 5 minute intervals to measure the power dissipated to the fluid, which can be done by using the equation below:

$$P(W) = mC_p \frac{dT}{dt}$$

Here the temperature is in Kelvin is taken with respect to time, P is the power (W), and Cp is the heat capacity of the solution. With this measurement the system efficiency can be calculated via the following:

$$Efficiency(\%) = \frac{Power\ Dissipated\ to\ Fluid}{Power\ Supplied\ to\ System}$$

The efficiency of the system is an important calculation for comparison between cavitational methods. The efficiency of the plate with the best iodine yield is displayed in Figure 20 below. Here, efficiency measurements were taken at cavitation numbers: 0.2, 0.22, and 0.24.

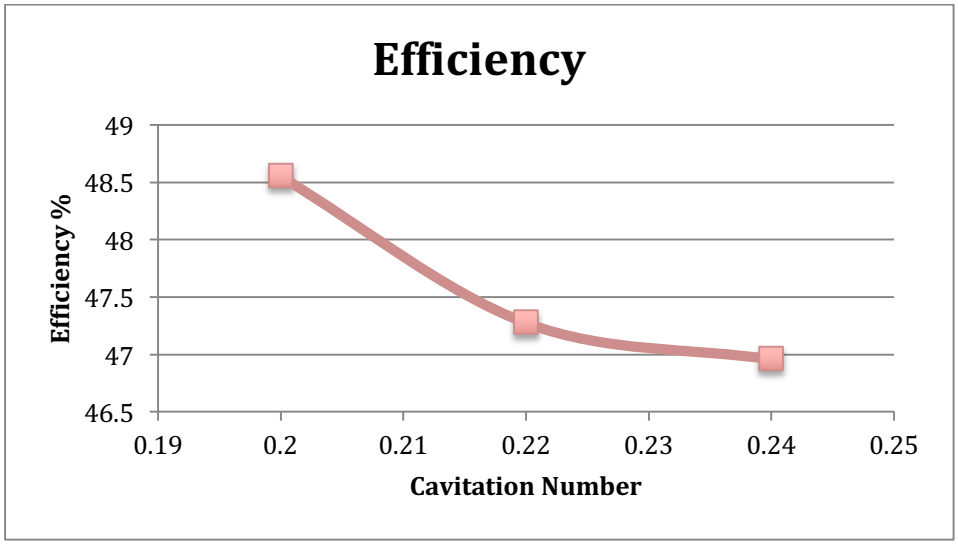

Figure 20 System Efficiency of Reactor Plate

The cavitational yield is the main parameter by which cavitating equipment is compared. With the varying methods of cavitation, including sonication and hydrodynamic, the cavitational yield is the baseline for comparison. The basic equation for calculating cavitational yield is given as follows:

$$Cavitational\ Yield = \frac{Iodine\ Liberated}{Power\ Density}$$

Here the calorimetric power density P(W) and the amount of iodine liberated (g/L) give the cavitational yield.

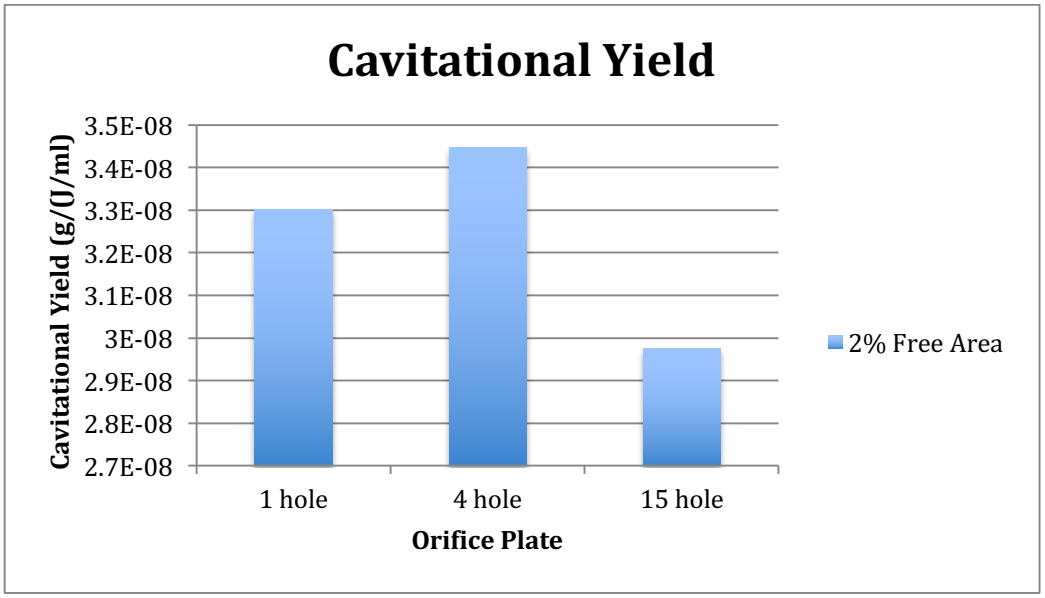

Figure 21 Cavitational Yield

4.4 Algal Disruption

Once the efficiency of the plate was determined and verified, the algae was run through the system at equivalent operating conditions. No processing was done to the algae sample prior to testing it in the reactor. Samples were taken before and after the solution was tested.

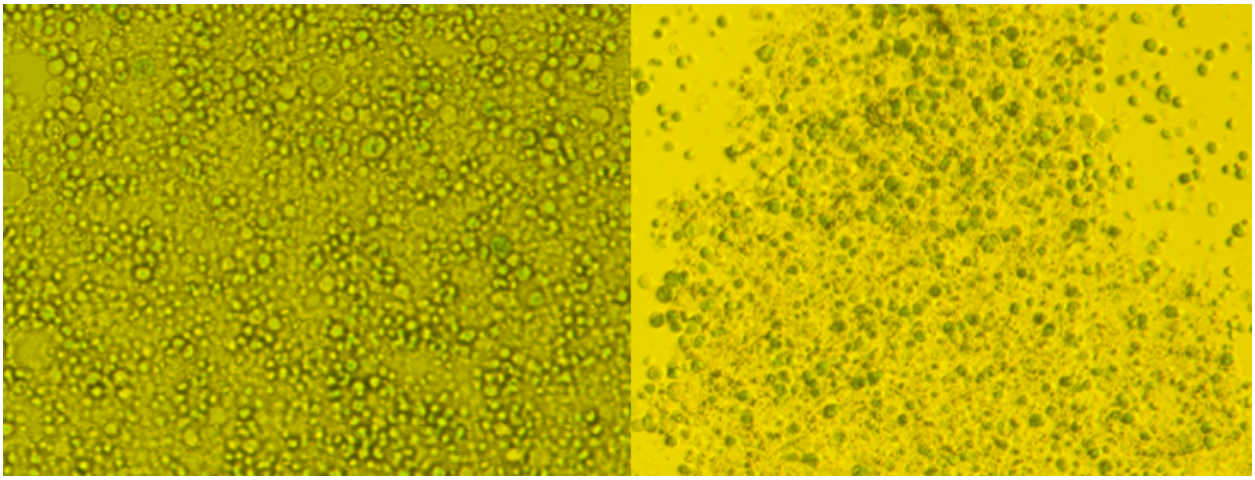

Figure 22 - Nannochloropsis before (left), and after (right) cavitation

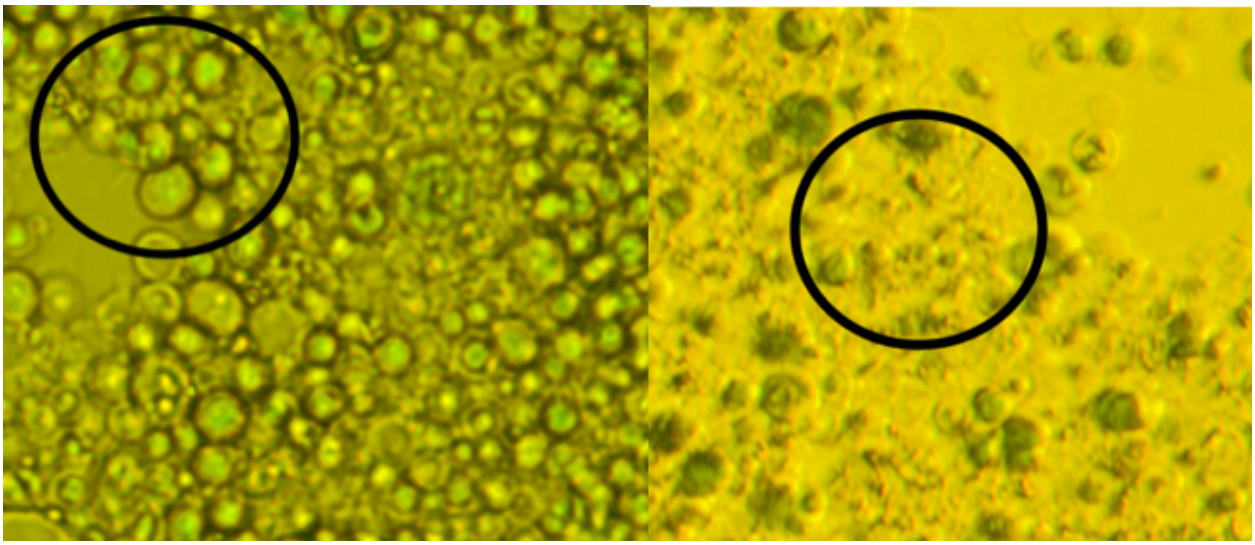

Figure 23 - Healthy (left) and Lysed microalgae

The figures above juxtapose the healthy and lysed algal cells, displaying disruptive effect that the hydrodynamic cavitation reactor had on the wet algal stream. The lysed algae, as

observed by optical microscopy, is shown on the right hand side of the image. Here, there are a few in tact algae cells but a majority are disrupted and the intracellular matter is separated from the cell.

Chapter 5

Concluding Remarks and Future Work

The preceding work is undertaken to understand effects of geometry on orifice plate design in a hydrodynamic cavitation reactor. While the geometry was shown to affect the iodine liberation rates, more work should be done in scaling the process. *Gogate et al. 2001* suggests that, due to its design and superior energy efficiency at pilot-plant scale, a scale up of the hydrodynamic cavitation system should increase efficiency further. The parameter introduced will aid in the design of orifice plate systems and may prove helpful when scaling of the hydrodynamic cavitation system. The effect of bulk fluid temperature on microbial cell disruption may be helpful as it is reported to affect the cavitational intensity.

Ultimately, the hydrodynamic cavitation reactor produced better energy efficiency than that of other physical disruption methods, including Dakshin bath and other forms of sonication. The system displayed iodine liberation rates above most other cavitation methods. This suggests that further work should be done to optimize and scale hydrodynamic cavitation as an energy efficient tool in cellular disruption. Scale up of the current work to a production sized system, where thousands of gallons could be processed in a day, would validate the use of this type of reactors usefulness in the field of sustainable biofuels.

The system displayed an ability to disrupt the algae cells, however the ability of the system to lyse the cell and fully release intracellular matter without damaging the lipid content was not investigated, and the usefulness of the end product as a source of biofuel was not able to be verified. Further, a total energy analysis, including the algal growth inputs such as water and nutrients, should be conducted for an end-to-end energy balance, making cavitation as a means

for cell disruption viable option as the need for alternative and sustainable forms of energy become necessary. As more work is done in engineering the strains of algae for higher lipid yield and more efficient biological growth, this method of biofuel processing will increasingly gain relevance in the world of sustainability.

Appendix

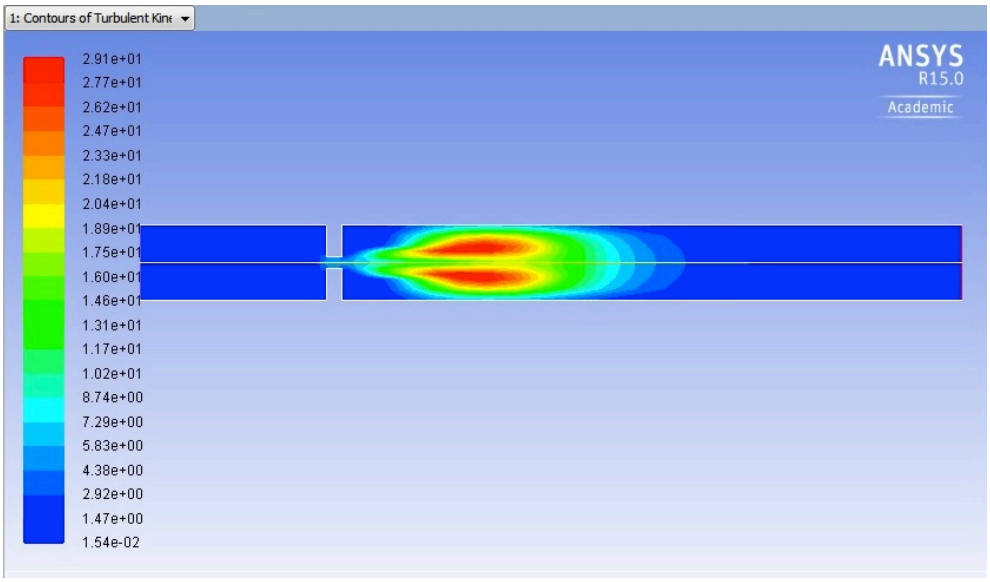

Figure 24 - Turbulent Kinteic Energy

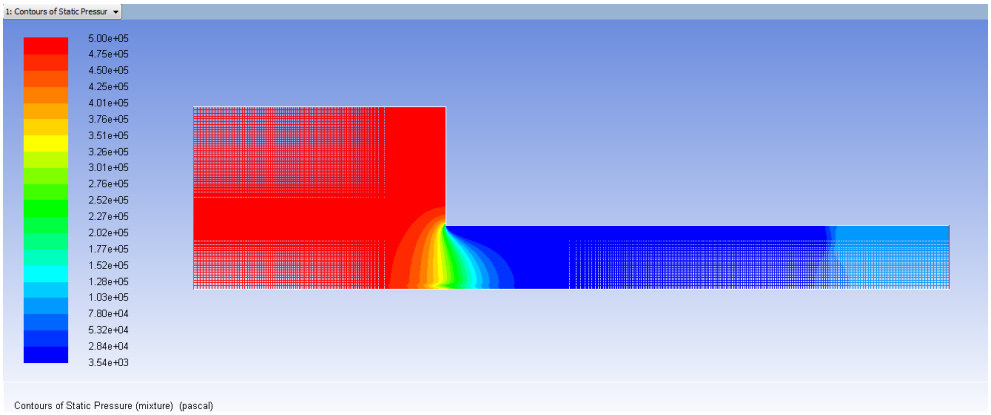

Figure 25 - Pressure Contours

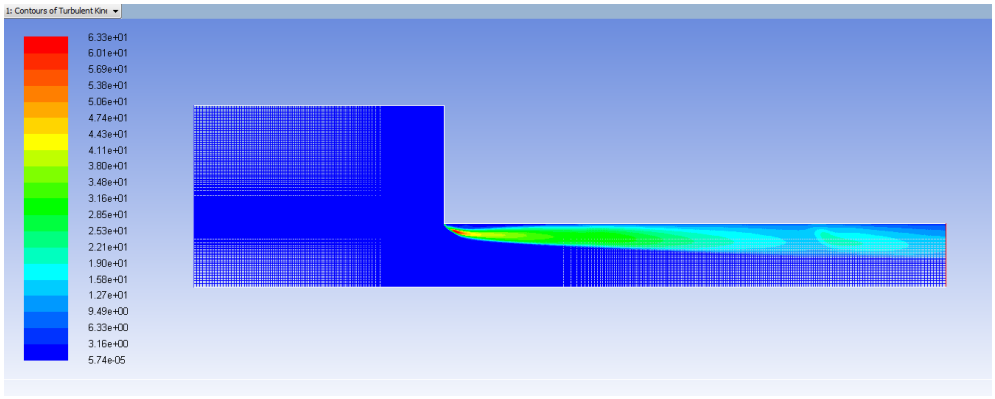

Figure 26 Turbulent Kinetic Energy (m^2/s^2)

Figure 27 - Cavitation Reactor: Side View

List of References

Anderson, Gary D. *Variable Frequency Drives: Installation and Troubleshooting*!. publication place: Createspace Independent Publishing Platform, 2013. Print.

Brennen, Christopher E. *Cavitation and Bubble Dynamics*. New York: Cambridge University Press, 2014. Print

Brennen, Liam, and Philip Owende. "Biofuels from Microalgae- A Review of Technologies for Production, Processing, and Extractions of Biofuels and co-products." *Renewable and Sustainable Energy Reviews* 14 (2010) 557-577. Print.

BP. BP Statistical Review of World Energy; 2014. Web.

Chun-Yen Chen, Kuei-Ling Yeh, Rifka Aisyah, Duu-Jong Lee, Jo-Shu Chang. "Cultivation, photobioreactor design and harvesting of microalgae for biodiesel production: A critical review." Bioresource Technology

Gogate, Parag R., A.B. Pandit. "A Review and Assesment of Hydrodynamic Cavitation as a Technology for the Future." *Ultrasonics Sonochemistry* 12 (2005) 21-27. Print.

Gogate, Parag R., I.Z. Shirgaonkar, M. Sivakumar, P. Senthilkumar, N.P. Vichare, and A.B. Pandit. "Cavitation Reactors: Efficiency Assessment Using a Model Reaction." *AIChE Journal* Vol. 47, No. 11 (2001) 2526-2538. Print.

Ho, Shih-Hsin, Chun-Yen Chen, Duu-Jong Lee, Jo-Shu Chang. "Perspectives on Microalgal CO2-Emission Mitigation Systems-A Review." *Biotechnology Advances* 29 (2011) 189-198. Print.

Franc, Jean-Pierre and Jean-Marie Michel. *Fundamentals of Cavitation*. Dordrecht, Netherlands: Kluwer Academic, 2004. Print.

ICCP, Climate Change 2013; 2013. Web.

Kumar, Kanhaiya, Chitralekha Nag Dasgupta, Bikram Nayak, Peter Linbald, Debabrata Das. "Development of Sustainable Photobioreactors for CO2 Sequestration Addressing Global Warming Using Green Algae and Cyanobacteria." *Bioresource Technology* 102 (2011) 4949-4953. Print.

Kumar, Kanhaiya, and Debabrata Das. "Growth Characteristics of Chlorella sorokiniana in Airlift Bubble Column Photobioreactors." Bioresource Technology 116 (2012) 307-313. Print.

Kumar, K. S., and V.S. Moholkar. "Conceptual Design of a Novel Hydrodynamic Cavitation Reactor." *Chemical Engineering Science* 62 (2007) 2698-2711. Print.

Kumar, P.S., M. Siva Kumar, A. B. Pandit. "Experimental Quantification of Chemical Effects of Hydrodynamic Cavitation." *Chemical Engineering Science* 55 (2000) 1633-1639. Print.

Lauterborn, W. "Cavitation and Coherent Optics." *Cavitation and Inhomogeneities in Underwater Acoustics.* Gottingen, Germany: Springer Berlin Heidelberg, 1980. Print.

Mata, Teresa M., Martins, Antonio A., and Nidia S. Caetano. "Microalgae for biodiesel production and other applications: A review." *Renewable and Sustainable Energy Reviews* 14.1-3 (2010): 217-232. Print.

Mercer, Paula, and Roberto Armenta. "Developments in Oil Extraction from Microalgae" *Eur. J. Lipid Sci. Technol.* (2011). Web.

Moholkar, V.S., P.S. Kumar, A.B. Pandit. "Hydrodynamic Cavitation for Sonochemical Effects." *Ultrasonics Chemistry* 6 (1999) 53-65. Print.

Morison, K.R., C.A. Hutchinson. "Limitations of the Weissler Reaction as a Model Reaction for Measuring the Efficiency of Hydrodynamic Cavitation." *Ultrasonics Chemistry* 16 (2009) 176-183. Print.

Pegallapati, Ambica Koushik, Y. Arudchelvam, N. Nirmalakhandan. "Energy-Efficient Photobioreactor Configuration for Algal Biomass Production." *Bioresource Technology* 126 (2012) 266-273. Print.

Posthuma, Adam Michael. *Microalgae Biofuel Production*. Masters Thesis. University Utrecht, Netherlands, 2009. Print.

Rastegary, J., Shirazi S. A., Fernandez T., Ghassemi A. "Water Resources for Algae-Based Biofuels." *Journal of Contemporary Water Research & Education* 151 (2013) 117-122. Print.

Sawant, S.S., Anil, A.C., Krishnamurthy, V., Chetan Gaonkar, Kolwalkar, J., Khandeparker, L., Desai, D., Mahulkar, A.V., Ranade, V.V., Pandit, A.B. "Effect of Hydrodynamic Cavitation on zooplankton: A tool for disinfection." *Biochemical Engineering Journal* 42 (2008) 320-328.

Singh, R.N., and Shaishav Sharma. "Development of Suitable Photobioreactor for Algae Production-A Review." *Renewable and Sustainable Energy Reviews* 16 (2012) 2347-2353. Print.

Shah, Yatish T., Pandit, A.B., and Moholkar, V.S. *Cavitation Reaction Engineering*. New York: Kluwer Academic/Plenum, 1999. Print.

Ugwu, C.U., H. Aoyagi, H. Uchiyama. "Photobioreactors for Mass Cultivation of Algae." *Biosource Technology* 99 (2008) 4021-4028. Print.

Vasumathi, K.K., M. Premalatha, P. Subramanian. "Parameters Influencing the Design of Photobioreactor for the Growth of Microalgae." *Renewable and Sustainable Energy Reviews* 16 (2012) 5443-5450. Print.

Wang, Bei, Christopher Q. Lan, and Mark Horsman. “Closed Photobioreactors for Production of Microalgal Biomasses.” *Biotechnology Advances* 30 (2012) 904-912. Print.

Young, F. Ronald. *Sonoluminescence*. Boca Raton: CRC Press, 2005. Print.

Zeiler K.G., Heacox D.A., Toon S.T., Kadam K.L., Brown L.M., Use of Microalgae for Assimilation and Utilization of Carbon Dioxide from Fossil Fuel-Fired Power Plant Flue Gas. Energy Conservation and Management 1995; 36(6-9): 107-12.

Curriculum Vitae

Christopher Caviglia was born and raised in El Paso, Texas. After graduating from El Paso High School in the top ten percent of his class, he attended the University of Texas at El Paso for his bachelors degree in mechanical engineering where he took interest in Society of Automotive Engineering, eventually becoming president of the organization. After receiving his bachelors degree in fall of 2013, he began research under Dr. Chianelli at the Materials Research and Technology Institute in sustainable biofuels.